Journal of Steroid Biochemistry & Molecular Biology 128 (2012) 154–164

Contents lists available at SciVerse ScienceDirect

Journal of Steroid Biochemistry and Molecular Biology

journal homepage: www.elsevier.com/locate/jsbmb

The liver X receptor modulator 22(S)-hydroxycholesterol exerts cell-type specific effects on lipid and glucose metabolism

Nina Pettersen Hessvik[a], Siril Skaret Bakke[a,1], Robert Smith[a,1], Aina Westrheim Ravna[b], Ingebrigt Sylte[b], Arild Christian Rustan[a], G. Hege Thoresen[a], Eili Tranheim Kase[a,*]

[a] Department of Pharmaceutical Biosciences, School of Pharmacy, University of Oslo, Oslo, Norway
[b] Medicinal Pharmacology and Toxicology, Department of Medical Biology, Faculty of Health Sciences, University of Tromsø, Tromsø, Norway

ARTICLE INFO

Article history:
Received 23 June 2011
Received in revised form
23 September 2011
Accepted 18 October 2011

Keywords:
Oxysterols
Liver X receptors
Nuclear receptors
Lipogenesis
Human cell models

ABSTRACT

The aim of this study was to explore the effects of 22(S)-hydroxycholesterol (22(S)-HC) on lipid and glucose metabolism in human-derived cells from metabolic active tissues. Docking of T0901317 and 22(S)-HC showed that both substances fitted into the ligand binding domain of liver X receptors (LXR). Results show that while several lipogenic genes were induced by T0901317 in myotubes, HepG2 cells and SGBS cells, effect of 22(S)-HC varied more between cell types. In myotubes, most lipogenic genes were downregulated or unchanged by 22(S)-HC, whereas a more diverse pattern was found in HepG2 and SGBS cells. Treatment with 22(S)-HC induced sterol regulatory element binding transcription factor 1 in SGBS and HepG2 cells, but not in myotubes. Fatty acid synthase was downregulated by 22(S)-HC in myotubes, upregulated in SGBS and unchanged in HepG2 cells. *De novo* lipogenesis was increased by T0901317 in all cell models, whereas differently affected by 22(S)-HC depending on the cell type; decreased in myotubes and HepG2 cells, whereas increased in SGBS cells. Oxidation of linoleic acid was reduced by 22(S)-HC in all cell models while glucose uptake increased and tended to increase in myotubes and SGBS cells, respectively. Cholesterol efflux was unaffected by 22(S)-HC treatment. These results show that 22(S)-HC affects LXR-regulated processes differently in various cell types. Ability of 22(S)-HC to reduce lipogenesis and lipid accumulation in myotubes and hepatocytes indicate that 22(S)-HC might reduce lipid accumulation in non-adipose tissues, suggesting a potential role for 22(S)-HC or a similar LXR modulator in the treatment of type 2 diabetes.

1. Introduction

Liver X receptors (LXR) are important regulators of cholesterol, lipid and glucose metabolism. These receptors are members of the nuclear receptor superfamily and regulate gene expression through interaction with LXR-responsive elements [1]. The LXRβ isoform is ubiquitously expressed in adults [2], whereas the expression of LXRα is mainly restricted to tissues known to play an important role in lipid metabolism, such as liver, adipose tissue, macrophages, kidney, skeletal muscle and small intestine [1,3,4]. Agonists for LXRs include naturally occurring oxidized cholesterol derivatives (oxysterols) [5] and the synthetic compound T0901317 [6], whereas the synthetic 22(S)-hydroxycholesterol (22(S)-HC) has been shown to act as a LXR antagonist on certain genes [7,8]. LXR agonists have been proposed as therapeutic agents for metabolic and cardiovascular diseases due to their effects on cholesterol [6,9] and glucose metabolism [10]. However, LXR activation mediates some undesirable effects, such as increased lipogenesis, hypertriglyceridemia and hepatic steatosis [6,10].

Increasing obesity promotes insulin resistance, but the location of body fat seems to be even more important than generalized adiposity for the disease development [11]. Recently, intrahepatic triacylglycerol content was shown to be a better predictor than visceral adipose tissue for metabolic disorders [12]. Ectopic fat deposition might lead to impaired organ function, and intracellular lipid content in skeletal muscle and liver correlates with insulin resistance and type 2 diabetes [11]. Therefore, antagonizing LXRs' effects on ectopic lipid accumulation might be beneficial in the treatment of type 2 diabetes.

Previously, we have shown that exposure to 22(S)-HC reduced synthesis of complex lipids, repressed certain genes involved in lipogenesis [7], and counteracted the T0901317-induced increase in lipid formation in human skeletal muscle cells [13]. 22(S)-HC reduced the activity of a reporter construct containing a LXR responsive element, supporting that 22(S)-HC

* Corresponding author at: Department of Pharmaceutical Biosciences, School of Pharmacy, University of Oslo, P.O. Box 1068 Blindern, N-0316 Oslo, Norway. Tel.: +47 22856545; fax: +47 22854402.
E-mail address: e.t.kase@farmasi.uio.no (E.T. Kase).
[1] Both the authors contributed equally to this study.

0960-0760/$ – see front matter © 2011 Elsevier Ltd. All rights reserved.
doi:10.1016/j.jsbmb.2011.10.006

regulates lipogenesis through direct interaction with LXRs [7]. Furthermore, 22(S)-HC increased glucose uptake and oxidation [13]. Thus, 22(S)-HC might have a therapeutic potential in the treatment of type 2 diabetes. We therefore wanted to investigate the effects of 22(S)-HC in human cell models representing metabolic active tissues important for development of type 2 diabetes. Significant differences in the response to LXR activation have been observed between human and rat hepatocytes, questioning the relevance of rodent models [14]. Few studies on effects of LXRs have been performed in human cells, thus such investigations are highly needed. The aim of the present study was to explore gene regulatory effects of 22(S)-HC compared to T0901317 in human myotubes, SGBS and HepG2 cells, representing human skeletal muscle, white adipose tissue and liver, respectively. Furthermore, we aimed to elucidate whether treatment with 22(S)-HC affected lipogenesis, fatty acid oxidation, glucose uptake and cholesterol efflux in these cells.

2. Materials and methods

2.1. Materials

Dulbecco's modified Eagle's medium (DMEM-Glutamax™, 5.5 and 25 mM glucose), DMEM without phenol red, foetal bovine serum, Ultroser G, penicillin–streptomycin–amphotericin B, and trypsin-EDTA were obtained from Gibco, Life Technologies (Paisley, UK). [1-^{14}C]acetic acid (54 mCi/mmol), [1-^{14}C]linoleic acid (56 mCi/mmol), [1-^{14}C]oleic acid (55 mCi/mmol), [1.2-^{3}H(N)]cholesterol (44.5 Ci/mmol) and 2-[^{3}H(G)]deoxy-D-glucose (6.0 Ci/mmol) were purchased from ARC (American Radiolabeled Chemicals, St. Louis, MO, USA). Insulin Actrapid was from Novo Nordisk (Bagsvaerd, Denmark). Linoleic acid, oleic acid, bovine serum albumin (BSA) (essentially fatty acid-free), extracellular matrix (ECM) gel, apoA1, DMEM/nutrient mix F-12 and 22(S)-hydroxycholesterol were purchased from Sigma–Aldrich (St. Louis, MO, USA). RNeasy Mini kit and RNase-free DNase were purchased from Qiagen Sciences (Oslo, Norway). Agilent Total RNA isolation kit was from Agilent Technologies (Santa Clara, CA, USA). The primers were purchased from Invitrogen (Paisley, Scotland, UK), while SYBR® Green and TaqMan® reverse-transcription reagents kit and TaqMan® Low Density Custom Arrays were from Applied Biosystems (Foster City, Canada). T0901317 was obtained from Cayman Chemical Company (Ann Arbor, MI, USA). Hydrophobic MultiScreen® HTS plates were from Millipore (Billerica, MA, USA). Corning® CellBIND® tissue culture plates were obtained from Corning Life-Sciences (Schiphol-Rijk, The Netherlands). OptiPhase Supermix and UniFilter®-96 GF/B were delivered by PerkinElmer (Shelton, CT, USA). Glass bottom plates were from MatTek (Ashland, MA, USA). The protein assay reagent was obtained from BioRad (Copenhagen, Denmark). MitoTracker®Red FM, Bodipy 493/503 (4,4-difluoro-1,3,5,7,8-pentamethyl-4-bora-3a,4a-diaza-s-indacene) and Hoechst 33258 were obtained from Molecular Probes, Invitrogen (Carlsbad, CA, USA). All other chemicals used were standard commercial high purity quality.

2.2. Docking experiment

The Internal Coordinate Mechanics program [15] was used for docking of 22(S)-HC and T0901317 into the ligand binding domain of the human LXRα and human LXRβ. The X-ray crystal structures of the LXRα ligand binding domain (PDB entry: 1UHL) and the LXRβ ligand binding domain (PDB entry: 1PQ6) were used as targets for docking of 22(S)-HC. The agonist T0901317 has been crystallized in complexes with LXRα (PDB entry: 1UHL) and LXRβ (PDB entry: 1PQ9). T0901317 was also docked into the ligand binding domains of LXRα and LXRβ, and the docking modes were compared with the X-ray crystallographic complexes.

The targets were converted to Internal Coordinate Mechanics objects, hydrogen atoms were added, and Grid maps were calculated based on ligand positions in the X-crystal structure complexes. A model of 22(S)-HC was generated using the Internal Coordinate Mechanics molecule editor and interactive flexible ligand docking was performed into the ligand binding domain of LXRα and LXRβ. The docking poses were grouped based on similarities in binding mode, and interaction energies were calculated using the calcBindingEnergy macro of Internal Coordinate Mechanics.

2.3. Cell culturing

2.3.1. Culturing of human myotubes

Satellite cells were isolated as previously described [16] from the *Musculus obliquus internus* abdominis of 6 healthy donors, age 39.9 (±2.9) years, body mass index 23.5 (±1.4) kg/m^2, fasting glucose 5.3 (±0.2) mM, insulin, plasma lipids and blood pressure within normal range and no family history of diabetes. The muscle biopsies were obtained with informed consent and approval by the National Committee for Research Ethics, Oslo, Norway. The cells were cultured in DMEM-Glutamax™ (5.5 mM glucose), 2% foetal bovine serum, 2% Ultroser G, penicillin (100 units/ml) and streptomycin (100 μg/ml), and amphotericin B (1.25 μg/ml) for proliferation. At 70–80% confluence the growth medium was replaced by DMEM-Glutamax™ (5.5 mM glucose) supplemented with 2% foetal bovine serum, penicillin (100 units/ml) and streptomycin (100 μg/ml), amphotericin B (1.25 μg/ml), and insulin (25 pM) to induce differentiation. The cells were cultured in humidified 5% CO_2 atmosphere at 37 °C, and the medium was changed every 2–3 days. Experiments were performed after 7 days of differentiation.

2.3.2. Culturing of SGBS cells

Human SGBS cells were cultured and differentiated into adipocytes as previously described [17]. Briefly, cells were seeded at low passage 6–10, cultured in basal medium (DMEM/nutrient mix F-12 supplemented with biotin (33 mM), D-pantothenate (17 mM), L-glutamine (2 mM), penicillin (100 units/ml) and streptomycin (100 μg/ml)) supplemented with 10% non-inactivated foetal bovine serum to confluence. For adipocyte differentiation, cells were exposed to adipogenic medium (basal medium supplemented with human transferrin (10 μg/ml), insulin (20 nM), cortisol (100 nM) and T3 (0.2 nM)) supplemented with dexamethasone (25 nM), isobutylmethylxanthine (0.5 mM) and rosiglitazone (2 μM) to increase differentiation rate for 4 days, followed by continuous culturing in adipogenic medium. Cortisol and T3 were removed from the medium during incubation with LXR ligands. The cells were cultured in humidified 5% CO_2 atmosphere at 37 °C, and medium was changed twice weekly until experiments were started at days 15–17.

2.3.3. Culturing of HepG2 cells

The human hepatoblastoma cell line HepG2 (HB-8065, ATCC, Manassas, VA, USA) was cultured in DMEM-Glutamax™ (5.5 mM glucose) supplemented with 10% foetal bovine serum, streptomycin (100 μg/ml) and penicillin (100 units/ml) at 37 °C in 5% CO_2.

2.3.4. Culturing of CaCo-2 cells

CaCo-2 cells obtained from American Type Culture Collection (Rockville, MD, USA) were grown in DMEM-Glutamax™ (25 mM glucose) supplemented with 20% foetal bovine serum, insulin (10 μg/ml), L-glutamine (2 mM), penicillin (50 units/ml), streptomycin (50 μg/ml) and 1% non-essential amino acids (BioWhittaker) and maintained as previously described [18]. For experiments, cells were plated at a density of 2×10^5 cells/cm^2 on 24 mm diameter collagen-treated cell culture filter inserts with

0.4 μm pore size (Corning® Transwell®-COL, Costar, Cambridge, MA, USA) and grown to 14 days post confluence. Cells were cultured in humidified 5% CO_2 atmosphere at 37 °C, and apical and basolateral media were changed three times a week.

2.4. RNA isolation and analysis of gene expression by TaqMan® low density custom arrays and real-time qPCR

After treatment with 1 μM T0901317, 10 μM 22(S)-HC or vehicle (0.1% DMSO) cells were harvested and total RNA was isolated by RNeasy Mini kit (Qiagen Sciences, Oslo, Norway) or Agilent Total RNA isolation kit (Agilent Technologies, Santa Clara, CA, USA) according to the supplier's total RNA isolation protocol. RNA samples were incubated with RNase-free DNase (Qiagen Sciences) for minimum 15 min in an additional step during the RNA isolation procedure. Equal amount of RNA obtained from myotubes from 4 different donors, SGBS-cells ($n = 4$), HepG2-cells ($n = 4$) and CaCo2-cells ($n = 4$) were reversely transcribed with a High Capacity cDNA Archive Kit. Each sample (100 ng/μl cDNA) was added to the slots of the array card and was run once on separate TaqMan® Low Density Custom Arrays according to the supplier's protocol (Applied Biosystems 7900HT, Low Density Custom Array, Getting started guide). A Low Density Custom Array was designed to analyze 93 genes involved in lipid and glucose metabolism. Glyceraldehyde-3-phosphate dehydrogenase (GAPDH) was used as reference gene and a fold change ≥2 or =0.5 was considered an increase or a decrease in expression level, respectively. For real-time qPCR, total RNA (1 μg/μl) was reversely transcribed with hexamere primers using a Perkin-Elmer Thermal Cycler 9600 (25 °C for 10 min, 37 °C for 1 h, 99 °C for 5 min) and a TaqMan reverse-transcription reagents kit (Applied Biosystems). Real-time PCR was performed on the same cDNA material used for the TDLA plates plus 1–2 more parallels using an ABI PRISM® 7000 Detection System. DNA expression was determined by SYBR® Green (Applied Biosystems). Primers (36B4, FASN, GAPDH and SREBF1) were designed using Primer Express® (Applied Biosystems). Primer sequences are available upon request. Each target gene were quantified in triplicates and carried out in a 25 μl reaction volume according to the supplier's protocol. All assays were run for 40 cycles (95 °C for 12 s followed by 60 °C for 60 s). The transcription levels were normalized to the reference control genes 36B4 and GAPDH.

2.5. Staining and live imaging of lipid droplets and mitochondria

Myotubes, SGBS and HepG2 cells were cultured as described above, with the exception of using 12-well glass bottom plates, coated with extracellular matrix gel for myotubes. The cells were treated with 1 μM T0901317, 10 μM 22(S)-HC or vehicle (0.1% DMSO) for 4 days (24 h for HepG2 cells). Myotubes, SGBS and HepG2 cells were incubated in 37 °C and 5% CO_2 with Bodipy 493/503 (2, 1 and 3 μg/ml, respectively) for 5–10 min to stain lipid droplets, Hoechst 33258 (2.5, 20 and 1.5 μg/ml, respectively) for 15–20 min to stain nuclei and MitoTracker®Red FM (100, 400 and 75 nM, respectively) for 15–25 min to stain mitochondria.

Automated image acquisition was performed in culture medium without phenol red with an ScanR̂ platform (Olympus IX81 inverted fluorescence microscope) equipped with a temperature and CO_2-enrichment incubator for long-term live imaging, as described in Hessvik et al. [19]. We used a 20× objective and live images of myotubes, SGBS and HepG2 cells were made at 25 (from 3 donors), 78 and 64 positions per well, respectively, and there were 3 wells per treatment. The background-subtracted maximal intensity projection from 7, 10 and 9 images taken in z-direction (1, 2 and 2 μm apart, respectively) was used for each colour channel at each position. One image contained about 35, 77 and 350 nuclei in average for myotubes, SGBS and HepG2 cells, respectively. HepG2 cells grew in layers and the first cell layer was also imaged separately to more easily quantify number of nuclei per image.

ScanR̂ software was used for automated image analysis, using edge detection algorithm for object segmentation to quantify the mitochondrial mass (intensity of MitoTracker®Red FM), and intensity, number and area of the lipid droplets (Bodipy 493/503), and number of nuclei per image. Lipid droplet volume was estimated from the measured diameter. Number of nuclei per image in HepG2 cells was determined from the intensity of Hoechst 33258 measured in all cell layers divided on the intensity from one nucleus. The SGBS cells were unevenly distributed in the wells and we restricted the data to the images with nucleus count between 50 and 100 per image to avoid possible effects of density. After excluding obvious artefactual abnormalities, each parameter was determined from 48 (one donor), 108 and 186 images per treatment for myotubes, SGBS and HepG2 cells, respectively.

2.6. Radiolabeled tracer studies

2.6.1. De novo lipogenesis

Cells were treated with 1 μM T0901317, 10 μM 22(S)-HC or vehicle (0.1% DMSO), before exposure to DMEM supplemented with [1-^{14}C]acetic acid (2 μCi/ml, 100 μM) for 4 h. Thereafter, cells were harvested in 0.2 M NaOH, assayed for protein [20] and total lipids were isolated by filtration of the cell lysate through hydrophobic MultiScreen® HTS plates (Millipore, Billerica, MA, USA). The levels of lipids were determined by scintillation counting, and lipogenesis from acetate was calculated by use of protein levels for standardization.

2.6.2. Fatty acid uptake and oxidation

Uptake and oxidation of linoleic acid was measured using an assay as previously described [21]. Briefly, after treatment with 1 μM T0901317, 10 μM 22(S)-HC or vehicle (0.1% DMSO), cells underwent CO_2 trapping for 4 h with [^{14}C]linoleic acid (1 μCi/ml, 100 μM). CO_2 and cell-associated radioactivity was measured by liquid scintillation and protein content was determined [20]. Acid-soluble metabolites were measured as previously described [22]. Uptake, acid-soluble metabolites and oxidation of linoleic acid were calculated by using protein levels for standardization. Similarly, using the same technique, uptake and oxidation of oleic acid was measured in myotubes during CO_2 trapping for 4 h with [^{14}C]oleic acid (1 μCi/ml, 100 μM) in the presence or absence of 5 mM glucose. Suppressibility, defined as the ability of the cells to decrease oleic acid oxidation by acutely added glucose, was calculated as: [(1−(oxidation of oleic acid at 5 mM glucose/oxidation of oleic acid at no glucose added)) × 100%] as previously described [19].

2.6.3. Glucose uptake

Cells were treated with 1 μM T0901317, 10 μM 22(S)-HC or vehicle (0.1% DMSO). Thereafter, cells were incubated for 20 min (37 °C, 5% CO_2) in serum-free DMEM containing 5.5 mM glucose, before addition of 2-[^{3}H(G)]deoxy-D-glucose (1 μCi/ml). Deoxyglucose uptake was measured after incubation in buffer containing 10 μM unlabelled deoxyglucose for 15 min. After incubation the cells were washed three times with ice-cold phosphate buffered saline (PBS), lysed in 0.05 M NaOH, and radioactivity was counted by liquid scintillation. Non-carrier mediated uptake was determined in the presence of cytochalasin B (5 μM) and subtracted from all presented values. The protein content of each sample was determined [20], and glucose uptake was calculated using protein levels for standardization.

2.6.4. Cholesterol efflux

Cells were exposed to either 1 μM T0901317, 10 μM 22(S)-HC or vehicle (0.1% DMSO) and prelabeled with [1,2-^{3}H(N)]cholesterol

(1 μCi/ml, 25 nM) for 48 h for myotubes, SGBS and CaCo-2 cells and for 24 h for HepG2 cells before efflux experiments were performed. Cells were washed twice with PBS and efflux of cholesterol was initiated in serum free medium in the presence or absence of 10 μg/ml apoA1. After 4 h, medium was removed, cell debris was pelleted and effluxed radioactivity was measured by scintillation counting. To obtain cell-associated [1.2-^{3}H(N)]cholesterol, cells were lysed in 0.2 M NaOH and radioactivity was measured by scintillation counting. Percent efflux was determined by dividing radioactivity in the culture media by the sum of radioactivity in the cell lysate and the media. ApoA1-dependent efflux was calculated by subtracting percent efflux without apoA1 from efflux with apoA1 present.

2.7. Presentation of data and statistical analysis

Data in text and figures are given as mean (±SEM) from n = number of separate experiments. For the data from the live imaging experiments, n = number of separate culture wells. Comparisons of different treatments were evaluated by ANOVA pairwise comparison with Bonferroni correction, and $P < 0.05$ was considered significant.

3. Results

3.1. Docking of T0901317 and 22(S)-HC into liver X receptors

The 22(S)-HC isomer has been shown to act as a LXR antagonist on certain genes [7,8]. To further verify the role of 22(S)-HC as an LXR modulator, we used the Internal Coordinate Mechanics program to study docking of 22(S)-HC, in comparison to the LXR agonist T0901317, into the ligand binding domains of LXRα and LXRβ. Docking of the agonist T0901317 into the ligand binding domain of LXRα gave a binding mode very similar to that observed in the X-ray structure (PDB entry: 1UHL) (Fig. 1A). Docking into LXRβ gave a docking mode that slightly diverged from the corresponding X-ray complex (Fig. 1B).

Based on previous X-ray crystallographic structures and molecular docking it has been suggested that interactions with His421 and Trp443 are important for forming an active complex for transcriptional regulation of liver X receptors [23]. As indicated in Fig. 1, these amino acids residues are conserved between LXRα and LXRβ, and such interactions are seen in the complexes of T0901317 with liver LXRα and LXRβ. Docking of 22(S)-HC showed that this compound occupied a space similar to that of T0901317 in both receptors (Fig. 1C and D). However, the hydroxyl group in 22-position was more shielded from direct interaction with the histidine and the tryptophan than the corresponding hydroxyl of T0901317 due to sterical hindrances in both receptors. This is in agreement with previous observations with LXRα [23].

3.2. Effects of 22(S)-HC treatment on genes regulating lipid metabolism in different human cell models

To explore gene regulatory effects of 22(S)-HC and T0901317 in various human cell models, mRNA analysis was performed by using TaqMan® Low Density Arrays and real-time PCR (Fig. 2). In human primary myotubes exposure to 22(S)-HC reduced or tended to reduce the expression of several genes involved in lipogenesis and lipid metabolism as LXRalpha, sterol regulatory element binding transcription factor 1 (SREBF1), stearoyl-CoA desaturase (SCD), fatty acid synthase (FASN), acetyl-Coenzyme A carboxylase α (ACACA), acyl-CoA synthetase long-chain family member 1 and 3 (ACSL1 and ACSL3), while, as previously reported [7,13,24] treatment with T0901317 increased the expression of these genes (Fig. 2A). Treatment of adipocytes (SGBS cells) with 22(S)-HC increased the expression of SREBF1, FASN and diacylglycerol O-acyltransferase homolog 1 (DGAT1), whereas SCD was reduced. In the same cells, exposure to T0901317 upregulated LXRα, SREBF1, ACACA and ACSL3, and downregulated DGAT1 expression (Fig. 2B). Moreover, in hepatocytes (HepG2 cells) 22(S)-HC treatment increased the expression of SREBF1, while T0901317 treatment increased the expression of SREBF1, SCD, FASN, ACACA and ACSL3 (Fig. 2C).

The expression of some of the lipogenic genes, SREBF1 and FASN, was confirmed by real-time RT-PCR analysis. Using this approach, 22(S)-HC treatment increased the expression of SREBF1 and FASN 3- and 2-fold, respectively, while T0901317 treatment of SGBS cells resulted in fold change of 3.6 and 0.74 for SREBF1 and FASN, respectively (Fig. 2D). In HepG2 cells, exposure to 22(S)-HC lead to 1.6- and 1.1-fold change for SREBF1 and FASN mRNA level while exposure to T0901317 resulted in fold change of 3.8 for SREBF1 and 3.7 for FASN (Fig. 2E). Gene expression was not confirmed by real-time RT-PCR in myotubes, since these data were in accordance with our previous findings [7,13,24].

Further, the cellular levels of LXRα and LXRβ were calculated by applying the ΔΔCt-method [25]. The mRNA expression of LXRα

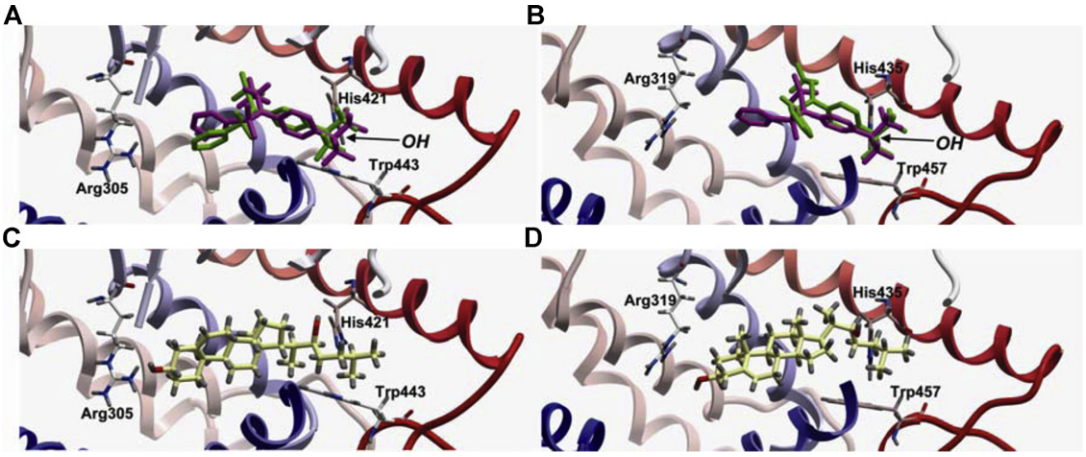

Fig. 1. Binding modes of T0901317 and 22(S)-HC in the ligand binding domain of LXRα and LXRβ. The Internal Coordinate Mechanics program was used for docking experiment as described in Section 2. T0901317 (green) docked into (A) LXRα and (B) LXRβ superimposed onto the corresponding X-ray structure (LXRα – PDB entry 1UHL and LXRβ – PDB entry 1PQ9). T0901317 from the corresponding X-ray complexes are shown in purple. The structure of 22(S)-HC docked into (C) LXRα and (D) LXRβ. Colour coding: Red O, blue N, grey H, yellow C in 22(S)-HC, white C in LXRα and LXRβ. Colouring of the Cα traces of LXRα and LXRβ is blue via white to red from N-terminal to C-terminal. (For interpretation of the references to color in this figure caption, the reader is referred to the web version of the article.)

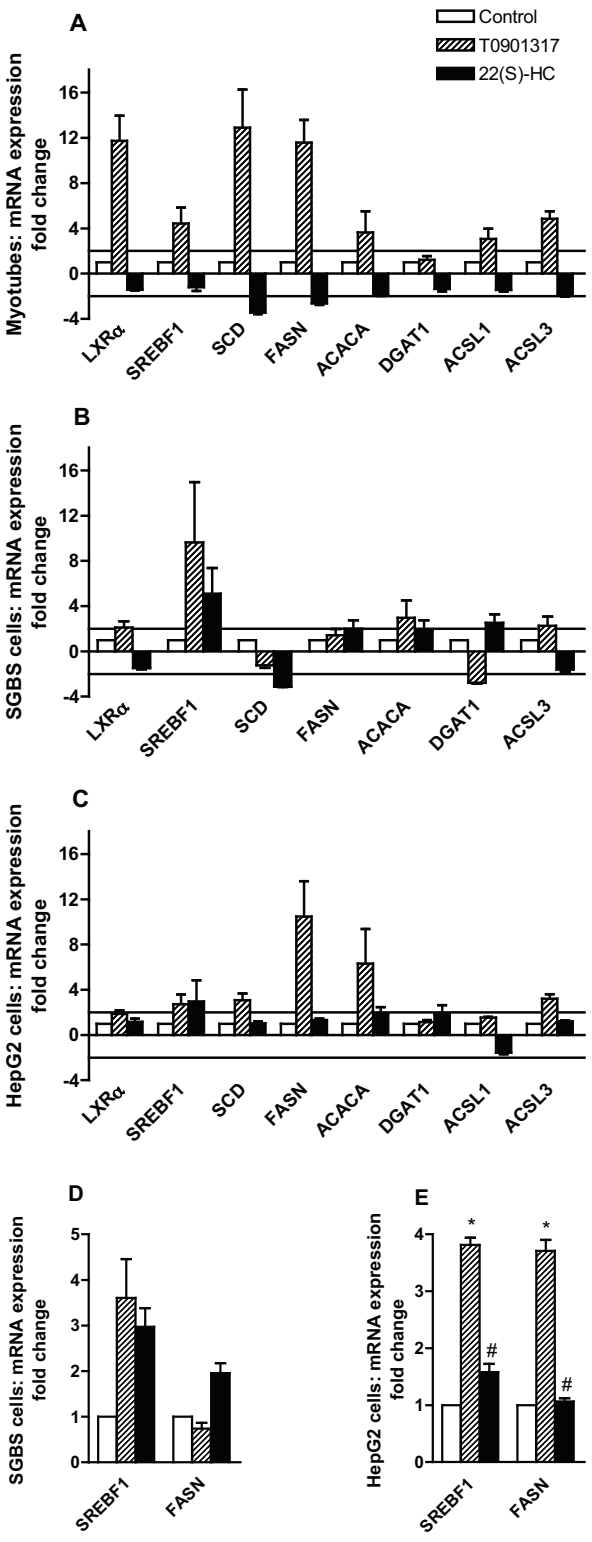

Fig. 2. Effects of 22(S)-hydroxycholesterol on genes involved in lipid metabolism in myotubes, SGBS and HepG2 cells. Cells were treated with 1 μM T0901317, 10 μM 22(S)-HC or DMSO (0.1%) for 4 days for myotubes and SGBS cells, and 24 h for HepG2 cells. Total RNA was isolated from the cells and analyzed by TaqMan® Low Density Custom Arrays or Real-Time PCR as described in Section 2. Gene expressions were normalized to levels of the reference gene glyceraldehyde-3-phosphate dehydrogenase (GAPDH). Selected genes involved in lipid metabolism in (A) myotubes, (B) SGBS cells and (C) HepG2 cells. Values represent fold change relative to control given as means ± SEM ($n = 4$). For genes with fold change < 1, fold change' is calculated as -1/fold change. Lines mark fold change = 2 and fold change = −2, the chosen cut-off for significance. Confirmatory Real-time data for (D) SGBS and (E) HepG2 represent fold change relative to control given as means ± SEM ($n = 5$–6). ACACA, acetyl-Coenzyme A carboxylase α; ACSL1/3, acyl-CoA synthetase long chain family member 1/3; DGAT1, diacylglycerol O-acyltransferase homolog 1; FASN, fatty acid synthase; LXRα, liver X receptor α; SCD, stearoyl-CoA desaturase; SREBF1, sterol regulatory element binding transcription factor 1.

was 1.5- and 2-fold higher than LXRβ in CaCo2 cells and HepG2 cells, respectively. However, these differences were not significant. The LXRα mRNA expression was about 550 times higher expressed than LXRβ in SGBS cells while LXRβ mRNA expression was about 15 times higher than LXRα in myotubes (data not shown).

3.3. Effects of 22(S)-HC treatment on lipogenesis and lipid accumulation

To examine whether the gene regulatory effects were reflected in corresponding endpoints of metabolic pathways, functional tracer studies were performed. *De novo* lipogenesis was dose-dependently reduced by 22SHC in HepG2 cells (Fig. 3A). Further, lipogenesis was differently affected by 22(S)-HC in various cell models. Treatment with 22(S)-HC reduced lipogenesis in both myotubes and HepG2 cells, whereas increased lipogenesis in SGBS cells (Fig. 3B). Contrary to 22(S)-HC, the LXR agonist T0901317 increased *de novo* lipogenesis from [^{14}C]acetate in all cell models (Fig. 3B).

Staining and quantification of lipid droplets by live cell imaging showed changes similar to what observed for lipogenesis (Fig. 3C). Exposure to 22(S)-HC did not affect the number of lipid droplets per nucleus in myotubes and SGBS cells, reduced the number of lipid droplets in HepG2 cells (Fig. 3C), while treatment with T0901317 increased the number of lipid droplets per nucleus in myotubes. The average volume of the lipid droplets in untreated cells was about 2.4, 144 and 1.5 μm^3 in myotubes, SGBS and HepG2 cells, respectively. The average volume of the lipid droplets in untreated cells was about 2.4, 140 and 1.5 μm^3 in myotubes, SGBS and HepG2 cells, respectively. The average lipid droplet volume and density (measured as fluorescence intensity per lipid droplet) was not affected by 22(S)-HC treatment in any of the cell types (data not shown), but was increased by 17% and 35% in myotubes ($P = 0.011$ and 0.012, respectively), and by 13% and 21% in HepG2 cells ($P = 0.007$ and 0.059, respectively) after T0901317-treatment. Neither of the two parameters were affected by T0901317 in SGBS cells.

3.4. Treatment with 22(S)-HC reduced linoleic acid oxidation

The acyl-CoA synthetase long-chain family (ACSL) members convert fatty acids to fatty acyl-CoA and play a key role in fatty acid oxidation [26–28]. To investigate whether the reduction in ACSL1 and 3 expression levels by 22(S)-HC treatment could be detected functionally, fatty acid oxidation (CO_2 production) was measured. We chose to use [^{14}C]linoleic acid since it is among the preferred substrates for ACSL3 [29] and also a good substrate for ACSL1 [26]. Fractional linoleic acid oxidation (oxidation of linoleic acid relative to linoleic acid uptake) was dose-dependently reduced by 22SHC in HepG2 cells (Fig. 4A). Further, fractional oxidation was reduced after 22(S)-HC treatment in all cell models examined (Fig. 4B). In contrast, after exposure to T0901317 the fractional oxidation was not changed in myotubes, tended to increase in SGBS cells ($P = 0.1$), and decreased in HepG2 cells (Fig. 4B). A similar trend was observed for oxidation of [^{14}C]palmitic acid, but not for oxidation of [^{14}C]oleic acid (data not shown). However, staining of mitochondria followed by live cell imaging showed no effect of 22(S)-HC treatment on mitochondrial mass in any of the cell models (data not shown).

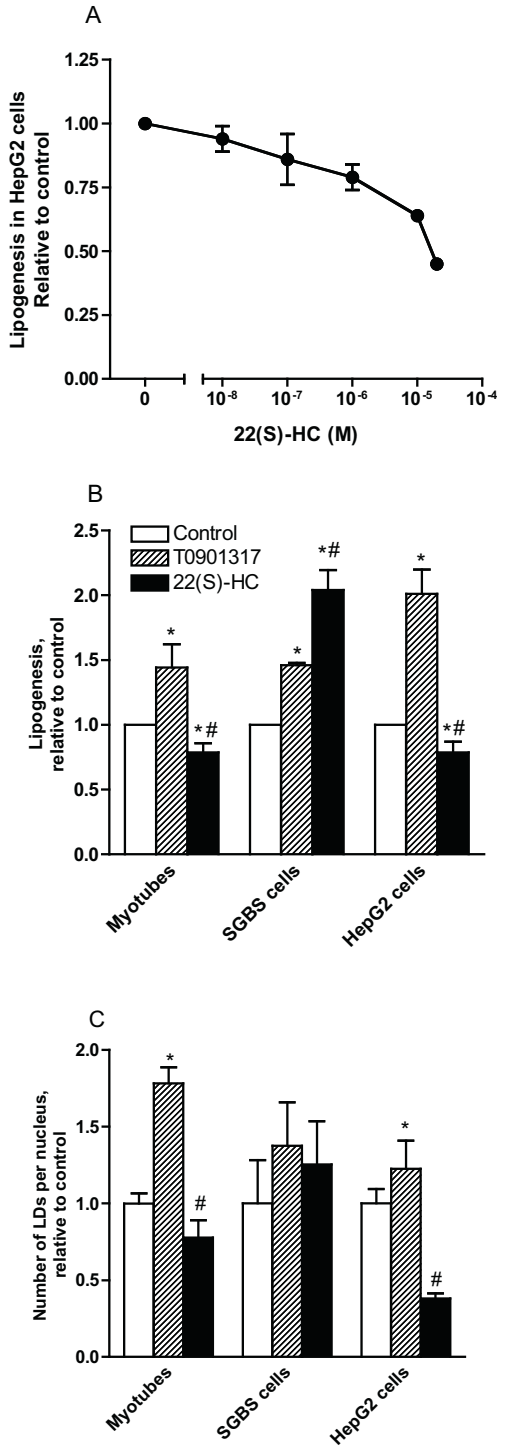

Fig. 3. Effects of 22(S)-hydroxycholesterol on lipogenesis and number of lipid droplets per nucleus in human myotubes, SGBS and HepG2 cells. Cells were treated with 1 μM T0901317, 0.01–20 μM 22(S)-HC or DMSO (0.1%) for 4 days for myotubes and SGBS cells, and 24 h for HepG2 cells. (A and B) *de novo* lipogenesis. The cells were incubated with [1-^{14}C]acetate (2 μCi/ml, 100 μM) for 4 h before lipids were isolated by filtration through hydrophobic MultiScreen® HTS plates. The levels of lipids were determined by scintillation counting. The ranges of the absolute values were 0.13–26.1, 70.2–547 and 2.2–43.3 nmol per mg cell protein for myotubes, SGBS and HepG2 cells, respectively. Values represent fold change relative to control for total lipids synthesized from acetate given as means ± SEM from (A) HepG2 cells, $n = 4$, and (B) $n = 5$–8 separate experiments. (C) Number of lipid droplets per nucleus. The cells were stained for lipid droplets and nuclei as described in Section 2. Results represent fold change relative to control given as means ± SEM, $n = 3$ wells, each value quantified from in average 16, 36 and 62 images per well for myotubes, SGBS and HepG2 cells, respectively. For myotubes; one representative donor out of three is presented. The ranges of the absolute values were 21–85, 5.2–13 and 1.5–7.0 lipid droplets per nucleus for myotubes, SGBS and HepG2 cells, respectively. $^{*}P < 0.05$ vs. control (DMSO) and $^{\#}P < 0.05$ for T0901317 vs. 22(S)-HC.

3.5. Treatment with 22(S)-HC increased glucose uptake in myotubes

Gene expression analysis revealed that none of the solute carrier family 2 (facilitated glucose transporter) members measured (SLC2A1, GLUT1; SLCA3, GLUT3; SLC2A4, GLUT4) were transcriptionally regulated after exposure to 22(S)-HC in myotubes, while T0901317 treatment upregulated SLCA4 (GLUT4) (Fig. 5A). In SGBS cells, exposure to 22(S)-HC induced SLC2A1, whereas T0901317 treatment upregulated SLC2A1 (GLUT1) and SLC2A3 (GLUT3) (Fig. 5B). SLC2A1 was also upregulated by 22(S)-HC treatment in HepG2 cells (Fig. 5C).

To further examine whether 22(S)-HC and T0901317 affected glucose metabolism, glucose uptake was measured. Exposure to 22(S)-HC increased basal glucose uptake in myotubes, tended to increase glucose uptake in SGBS cells, but had no effect on this process in HepG2 cells (Fig. 6A). Furthermore, 22(S)-HC was found to increase glucose uptake in a concentration-dependent manner in myotubes (Fig. 6B). Treatment with T0901317 increased basal glucose uptake in SGBS and HepG2 cells, but did not affect this process in myotubes (Fig. 6A).

3.6. Effects of 22(S)-HC treatment on glucose suppressibility of fatty acid oxidation

Skeletal muscle of lean, healthy individuals is metabolically flexible; is capable of easily switching from predominantly lipid oxidation during fasting to glucose oxidation in the postprandial state [30]. Loss of this ability is termed metabolic inflexibility [30], and is linked to obesity and type 2 diabetes [31]. To investigate whether treatment with 22(S)-HC affected metabolic switching in myotubes, suppressibility, defined according to Ukropcova et al. as the ability of myotubes to decrease oleic acid oxidation by acute addition of glucose (5 mM) [32], was studied. We recently showed that treatment of myotubes with T0901317 did not affect suppressibility *per se* [19]. Contrarily, treatment with 22(S)-HC increased suppressibility of myotubes by 2.5-fold compared to control cells (Fig. 6C).

3.7. Treatment with 22(S)-HC did not negatively influence cholesterol metabolism

The ATP-binding cassette transporters (ABC) are well-known LXR target genes, and were also investigated in this study. A cell model representing intestinal cells (CaCo-2 cells) was also included in these experiments. ABCA1 was upregulated by T0901317-treatment in all cell models examined (Fig. 7A). Exposure to 22(S)-HC also induced ABCA1 in myotubes and CaCo-2 cells, but to a much lesser extent compared to T0901317 (Fig. 7A). Another ABC transporter, ABCG1, was upregulated by both 22(S)-HC and T0901317 in SGBS and CaCo-2 cells, however to a much higher degree by T0901317 (Fig. 7B).

To investigate whether 22(S)-HC could exert a negative effect on cholesterol metabolism, apoA1-dependent cholesterol efflux was measured. Exposure to 22(S)-HC did not affect apoA1-dependent cholesterol efflux in myotubes, HepG2 or CaCo-2 cells, but tended to increase apoA1-dependent cholesterol efflux in SGBS cells ($P = 0.1$). As expected, treatment with T0901317 increased apoA1-dependent cholesterol efflux in myotubes and SGBS cells, whereas no effect was seen in HepG2 cells (Fig. 7C). For CaCo-2 cells, T0901317-treatment increased and tended to increase

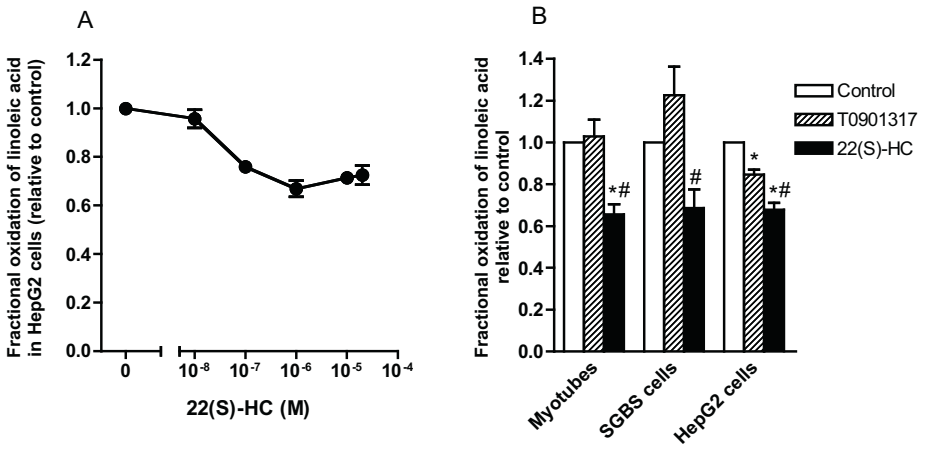

Fig. 4. 22(S)-hydroxycholesterol reduces fractional oxidation of linoleic acid in myotubes, SGBS and HepG2 cells. Cells were treated with 1 μM T0901317, 0.01–20 μM 22(S)-HC or DMSO (0.1%) for 4 days for myotubes and SGBS cells, and 24 h for HepG2 cells. Thereafter, the cells underwent CO_2 trapping for 4 h with [^{14}C]linoleic acid (1 μCi/ml, 100 μM) as described in Section 2. [^{14}C]CO_2 was counted by liquid scintillation. Cells were assayed for protein content, cell-associated linoleic acid, acid-soluble metabolites and linoleic acid oxidation were calculated by using protein levels for standardization. Fractional oxidation was calculated as amount CO_2 divided by total uptake of linoleic acid. The ranges of the absolute values of linoleic acid oxidation were 1.2–6.2, 1.7–4.7 and 7.4–15.1 nmol per mg cell protein for myotubes, SGBS and HepG2 cells, respectively. Values represent (A) a dose–response curve in HepG2 cells representing one of two independent experiments ($n = 4$ wells) and (B) fold change relative to control shown as means ± SEM ($n = 5$–7 separate experiments). $^{*}P < 0.05$ vs. control (DMSO) and $^{\#}P < 0.05$ for T0901317 vs. 22(S)-HC.

apoA1-dependent cholesterol efflux from the cells to the basolateral side (representing "blood" side) and to the apical side representing intestinal lumen, respectively (Fig. 7D).

4. Discussion

This study provides novel information on the effects of pharmacological modulation of LXRs in human cell models, and is the first to show that several effects of 22(S)-hydroxycholesterol (22(S)-HC) depend on the cell type examined. Several genes in lipid metabolism were differently regulated by 22(S)-HC and T0901317 in various human cell models, and this was reflected by corresponding functional endpoints in metabolic pathways.

Docking of T0901317 and 22(S)-HC showed that both substances fitted into the ligand binding domain of LXRα, in line with previous findings [23]. In addition, we showed similar results for docking of these substances into ligand binding domain of LXRβ. The hydroxyl group in 22-position on 22(S)-HC was more shielded from direct interaction with histidine and tryptophan than the corresponding hydroxyl of T0901317 due to sterical hindrances in both receptors. These amino acids have previously been indentified by mutagenesis as critical for ligand-induced transcriptional activation by T0901317 [23]. This might indicate that 22(S)-HC has different properties for generating a transcription complex and might serve as an antagonist.

The mRNA level of sterol regulatory element binding transcription factor 1 (SREBF1) was increased by 22(S)-HC in SGBS and HepG2 cells, but not in myotubes, however induced by T0901317 in all cell models, in accordance with previous studies [24,33,34]. Treatment with 22(S)-HC reduced the mRNA level of fatty acid synthase (FASN) in myotubes, as previously shown [7,13], whereas increased FASN expression in SGBS cells. In HepG2 cells 22(S)-HC did not affect FASN mRNA level. T0901317 upregulated FASN in myotubes and HepG2 cells, in accordance with previous findings [7,35]. In contrast to a previous study using murine adipocytes [33], FASN level was unaffected by T0901317 in SGBS cells. The expression of diacylglycerol O-acyltransferase homolog 1 (DGAT1), the enzyme that catalyze the final step in synthesis of triacylglycerol, was only affected in SGBS cells, in which 22(S)-HC increased the expression, while T0901317 reduced it.

The regulatory effects of 22(S)-HC and T0901317 on genes in lipid metabolism were in line with the functional outcome of *de novo* lipogenesis and lipid accumulation. The observed effects in myotubes, in which 22(S)-HC reduced, whereas T0901317 increased *de novo* lipogenesis, are in accordance with previous findings [7]. Treatment with 22(S)-HC reduced *de novo* synthesis of lipids similarly in HepG2 cells as in myotubes. Contrary, in SGBS cells, this process was increased after 22(S)-HC exposure. Treatment with T0901317 increased *de novo* synthesis of lipids from acetate in myotubes, SGBS cells and HepG2 cells.

In accordance with the responses on *de novo* lipogenesis, 22(S)-HC decreased the number of lipid droplets in HepG2 cells, whereas had no significant effect on this parameter in myotubes and SGBS cells. The finding in SGBS cells is in contrast to a report by Juvet et al. indicating that murine 3T3-L1 cells treated with 22(S)-HC accumulated less lipids compared to control cells [33]. The discrepancy between these studies could be due to specie or methodological differences. Kotokorpi et al. showed several dissimilarities in LXR responses between human and rat hepatocytes, signifying the need for such studies in human cell models [14].

We observed that treatment with 22(S)-HC decreased linoleic acid (LA) oxidation in all cell models examined. This might indicate an undesirable effect of 22(S)-HC, since decreased fatty acid oxidation is associated with development of type 2 diabetes (T2D) [36,37], and previous studies have shown that myotubes established from T2D subjects had a lower palmitic acid oxidation relative to myotubes established from healthy controls [38,39]. However, oxidation of oleic acid was not reduced by 22(S)-HC treatment. This may indicate that effects of 22(S)-HC on lipid oxidation vary with type of fatty acid. Glucose uptake and oxidation was also increased by 22(S)-HC treatment [13]. Both the increase in glucose uptake and decline in LA oxidation could be secondary to increased glucose oxidation, while reduced LA oxidation may also be due to decreased lipid accumulation. Furthermore, treatment with 22(S)-HC did not alter the mitochondrial mass in any of the cell models, hence the reduced LA oxidation might not indicate a detrimental effect of 22(S)-HC.

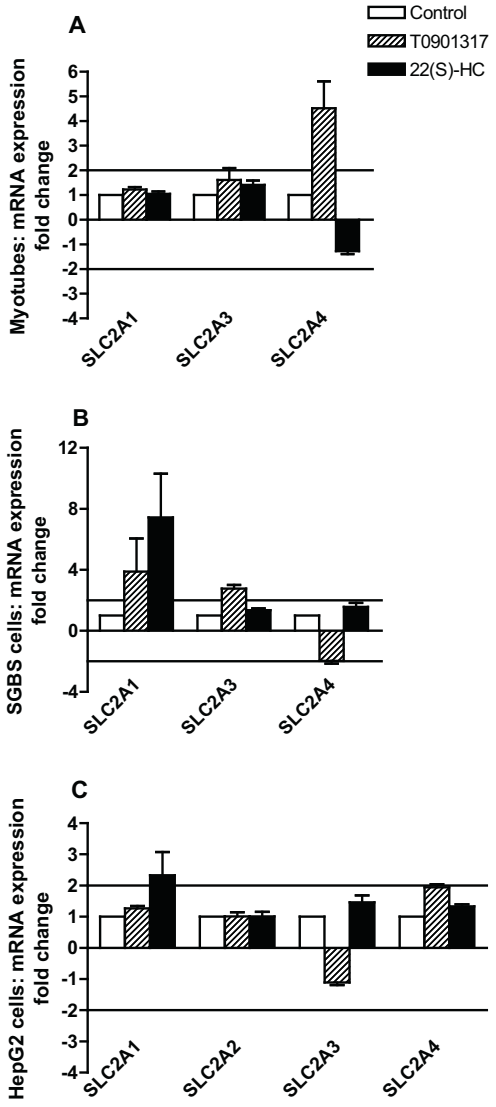

Fig. 5. Effects of 22(S)-hydroxycholesterol on expression level of glucose transporters in myotubes, SGBS and HepG2 cells. Cells were treated with 1 μM T0901317, 10 μM 22(S)-HC or DMSO (0.1%) for 4 days for myotubes and SGBS cells, and 24 h for HepG2 cells. Total RNA was isolated from the cells and analyzed by TaqMan® Low Density Custom Arrays as described in Fig. 1 for SGBS and HepG2 cells. mRNA level was measured by real-time RT-PCR in myotubes, as described in Section 2. Values represent fold change relative to control given as means ± SEM ($n = 4$) for glucose transporters (GLUT) in (A) myotubes, (B) SGBS cells and (C) HepG2 cells. For genes with fold change < 1, fold change' is calculated as −1/fold change. Lines mark fold change = 2 and fold change = −2, the chosen cut-off for significance. SLC2A1-4, solute carrier family 2 (facilitated glucose transporter), member 1–4 (GLUT1–4).

In the present study exposure to 22(S)-HC and T0901317 did not show major impact on the expression level of glucose transporters. Some stimulating effect on glucose uptake was observed, but this only reflected the gene regulatory pattern in SGBS cells. Thus, the mechanisms by which 22(S)-HC and T0901317 affect glucose uptake may not be explained by changes in the expression level of glucose transporters, and remain unknown.

Metabolic inflexibility, which is defined as loss of the ability to switch easily from predominantly lipid oxidation during fasting to glucose oxidation in the postprandial state [30], is linked to obesity and type 2 diabetes [31]. A study by Ukropcova et al. indicated that metabolic switching could be an intrinsic characteristic of human skeletal muscle cells [32]. Since LXRs regulate lipid and glucose metabolism, 22(S)-HC treatment might affect this switching. We recently showed that suppressibility of myotubes, defined as the ability of acutely added glucose to suppress fatty acid oxidation, was not affected by LXR activation by T0901317 *per se* [19]. However, the *n*-3 fatty acid eicosapentaenoic acid increased suppressibility, and treatment with T0901317 cancelled out this effect [19]. In the present study we showed that 22(S)-HC treatment of myotubes increased suppressibility. This indicates a certain role for LXRs in metabolic switching and a potential beneficial effect of 22(S)-HC improving metabolic switching of skeletal muscle.

LXRs regulate reverse cholesterol transport through several mechanisms, mainly through regulation of members of the ABC superfamily. In the present study we observed that T0901317-treatment induced ABCA1 in myotubes, SGBS, HepG2 and CaCo-2 cells, as well as ABCG1 in SGBS and CaCo-2 cells, in accordance with previous reports [7,40–42]. Due to the beneficial effects of LXR activation on cholesterol homeostasis, LXR antagonists could be suspected to exert a negative effect on whole body cholesterol homeostasis. However, 22(S)-HC induced ABCA1 in myotubes and CaCo-2 cells, in addition to ABCG1 in SGBS and CaCo-2 cells.

ApoA1-dependent cholesterol efflux was regulated by the LXR modulators in a similar pattern as ABCA1 and ABCG1 gene expression. Treatment with T0901317 increased apoA1-dependent cholesterol efflux from human myotubes, as well as SGBS and CaCo-2 cells. We did not observe LXR-mediated elevation of apoA1-dependent cholesterol efflux from HepG2 cells, contrary to a previous report [40]. LXR activation has previously been shown to enhance apoA1-dependent cholesterol efflux from murine myotubes [22], HepG2 cells [40], murine 3T3-L1 adipocytes [42] and basolateral cholesterol efflux from CaCo-2 cells [41], but has not, to our knowledge, been studied in human adipocytes or myotubes. The effect of 22(S)-HC on cholesterol efflux has not previously been investigated. Exposure to 22(S)-HC did not alter apoA1-dependent cholesterol efflux in myotubes, HepG2 or CaCo-2 cells, but tended to increase efflux from SGBS cells.

Tissue-selective regulation by LXRs, as we observed for some genes and metabolic processes, is also reported earlier for certain genes. The explanation for this specificity is unknown, but several mechanisms might contribute. Unequal tissue distribution of the two LXR subtypes combined with different gene regulation by these receptors could result in tissue-selective effects. Furthermore, differential regulation of target genes could also be due to distinct coactivator and corepressor recruitment. This is reported to occur for ABCA1 and SREBF1 [43]. Also, variation in the level and type of coactivators or corepressors within distinct tissues might contribute to the specificity. However, this needs further investigation. Some of the effects of 22(S)-HC could also be due to LXR-independent mechanisms, since oxysterols exert some effects independently of LXRs [44]. These effects could be mediated through interaction with other transcription factors or oxysterol-sensing proteins, or through post-translational modifications [45]. Furthermore, some of the observed effects after T0901317-treatment might be mediated through other nuclear receptors than LXRs, since this ligand has been shown to be an agonist or inverse agonist on farnesoid X receptor, pregnane X receptor and retinoic acid receptor-related orphan receptors in some cell models [46–48].

In conclusion, our study showed that 22(S)-HC, likely through interacting with LXRs, differently affects lipid and glucose metabolism depending on the cell model examined. The ability of 22(S)-HC to reduce lipogenesis and lipid accumulation in myotubes and hepatocytes indicate that 22(S)-HC might reduce lipid accumulation in non-adipose tissues, suggesting a potential role for 22(S)-HC or a similar LXR modulator in the treatment of

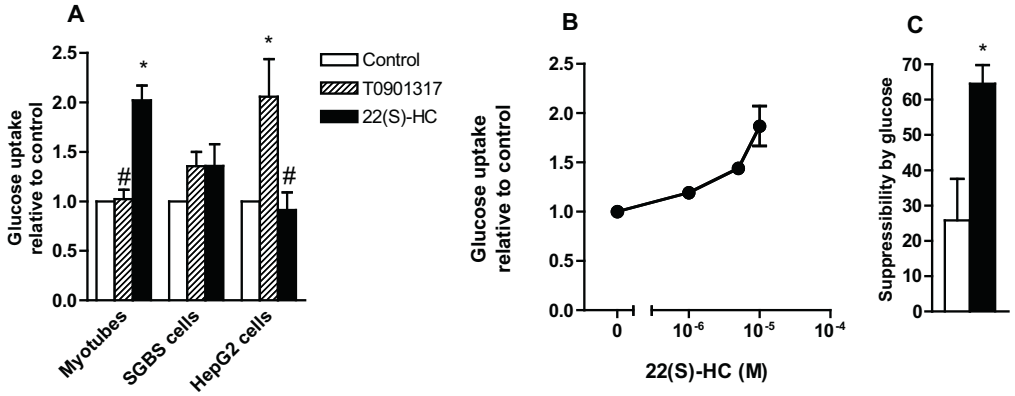

Fig. 6. 22(S)-hydroxycholesterol increases glucose uptake in myotubes. (A) Glucose uptake. Cells were treated with 1 μM T0901317, 10 μM 22(S)-HC or DMSO (0.1%) for 4 days for myotubes and SGBS cells, and 24 h for HepG2 cells. Thereafter, the cells were incubated for 20 min in serum-free DMEM containing 5.5 mM glucose, before addition of 2-[^{3}H(G)]deoxy-D-glucose (1 μCi/ml). After 15 min incubation the cells were lysed in NaOH, and radioactivity was counted by liquid scintillation. Cells were assayed for protein and glucose uptake was calculated by using protein levels for standardization. Values represent fold change relative to control shown as means ± SEM (n = 4–6). The ranges of the absolute values were 35.0–182, 6.6–29.9 and 0.28–35.2 pmol/mg cell protein/min for myotubes, SGBS and HepG2 cells, respectively. (B) Dose–response of 22(S)-HC in myotubes. Myotubes were exposed to 0, 1, 5 and 10 μM of 22(S)-HC for 4 days before glucose uptake was measured as described above. Values represent fold change relative to control shown as means ± SEM (n = 3). (C) Suppressibility by glucose in myotubes. Myotubes were treated for 4 days with 10 μM 22(S)-HC or DMSO (0.1%), and thereafter underwent CO_2 trapping for 4 h with [^{14}C]oleic acid (1 μCi/ml, 100 μM) in the presence or absence of 5 mM glucose as described in Section 2. Suppressibility, the ability of the cells to decrease oleic acid oxidation by glucose, was calculated as [(1-(oxidation of oleic acid at 5 mM glucose/oxidation of oleic acid at no glucose added)) × 100%]. Results represent means ± SEM from 5 different donors. *P < 0.05 vs. control (DMSO) and #P < 0.05 for T0901317 vs. 22(S)-HC.

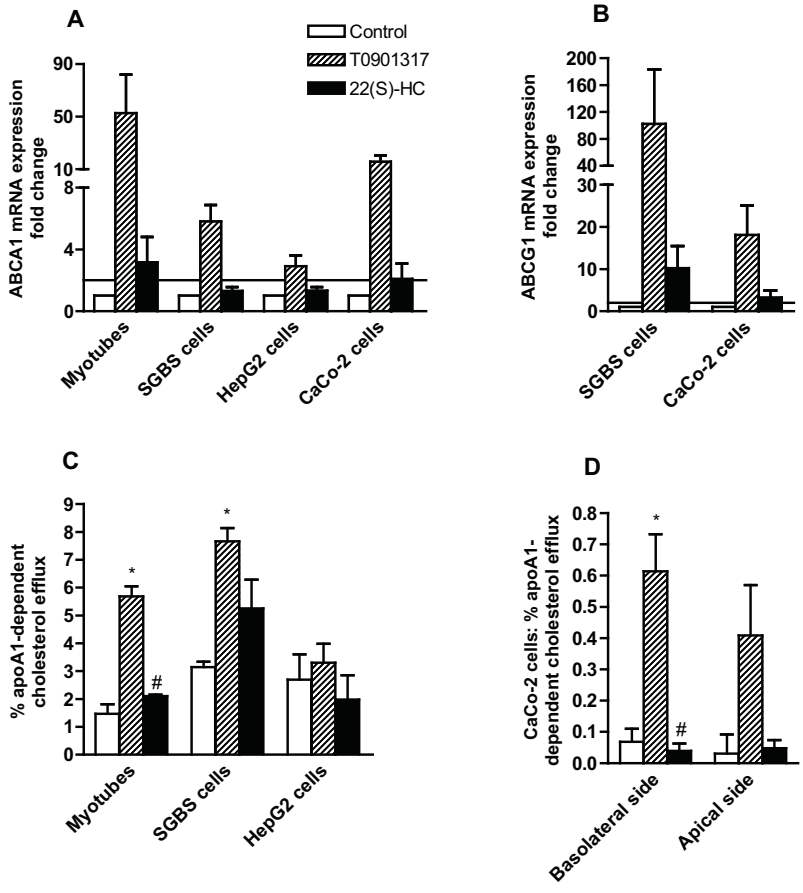

Fig. 7. 22(S)-hydroxycholesterol does not negatively influence cholesterol efflux in myotubes, SGBS, HepG2 and CaCo-2 cells. (A and B) mRNA levels of ATP-binding cassette transporter A1 (ABCA1) and ABCG1, respectively. Cells were treated with 1 μM T0901317, 10 μM 22(S)-HC or DMSO (0.1%) for 4 days for myotubes and SGBS cells, and 24 h for HepG2 cells. Total RNA was isolated from the cells and analyzed by TaqMan® Low Density Custom Arrays as described in Fig. 1. Values represent fold change relative to control given as means ± SEM (n = 4). Line marks fold change = 2, the chosen cut-off for significance. (C and D) Cells were treated with 1 μM T0901317, 10 μM 22(S)-HC or DMSO (0.1%) for 48 h for myotubes, SGBS and CaCo-2 cells, and 24 h for HepG2 cells. Thereafter, the cells were prelabeled with [1.2-^{3}H(N)]cholesterol (1 μCi/ml, 25 nM) and still exposed to T0901317, 22(S)-HC or DMSO for another 2 days. The cells were incubated with or without apoA1 (10 μg/ml) for 4 h, before radioactivity in the medium and cell lysate was determined by scintillation counting as described in Section 2. % apoA1-dependent cholesterol efflux from (C) myotubes, SGBS cells and HepG2 cells and (D) CaCo-2 cells to basolateral (blood) and apical (intestinal lumen) side. Values represent fold change relative to control given as means (n = 4–5). *P < 0.05 vs. control (DMSO) and #P < 0.05 for T0901317 vs. 22(S)-HC.

type 2 diabetes. However, more studies, including *in vivo* studies, are necessary to further explore the metabolic effects of 22(S)-HC.

Acknowledgements

This work was supported by University of Oslo. We want to thank Dr. Gerbrand Koster and Prof. Oddmund Bakke at the NORMIC-UiO imaging platform at Department of Molecular Biosciences, University of Oslo, for support and use of equipment, and Anne Randi Enget for excellent technical assistance.

References

[1] P.J. Willy, K. Umesono, E.S. Ong, R.M. Evans, R.A. Heyman, D.J. Mangelsdorf, LXR, a nuclear receptor that defines a distinct retinoid response pathway, Genes Dev. 9 (9) (1995) 1033–1045.
[2] C. Song, J.M. Kokontis, R.A. Hiipakka, S. Liao, Ubiquitous receptor: a receptor that modulates gene activation by retinoic acid and thyroid hormone receptors, Proc. Natl. Acad. Sci. U. S. A. 91 (23) (1994) 10809–10813.
[3] R. Apfel, D. Benbrook, E. Lernhardt, M.A. Ortiz, G. Salbert, M. Pfahl, A novel orphan receptor specific for a subset of thyroid hormone-responsive elements and its interaction with the retinoid/thyroid hormone receptor subfamily, Mol. Cell Biol. 14 (10) (1994) 7025–7035.
[4] D. Auboeuf, J. Rieusset, L. Fajas, P. Vallier, V. Frering, J.P. Riou, B. Staels, J. Auwerx, M. Laville, H. Vidal, Tissue distribution and quantification of the expression of mRNAs of peroxisome proliferator-activated receptors and liver X receptor-alpha in humans: no alteration in adipose tissue of obese and NIDDM patients, Diabetes 46 (8) (1997) 1319–1327.
[5] B.A. Janowski, P.J. Willy, T.R. Devi, J.R. Falck, D.J. Mangelsdorf, An oxysterol signalling pathway mediated by the nuclear receptor LXR alpha, Nature 383 (6602) (1996) 728–731.
[6] J.R. Schultz, H. Tu, A. Luk, J.J. Repa, J.C. Medina, L. Li, S. Schwendner, S. Wang, M. Thoolen, D.J. Mangelsdorf, K.D. Lustig, B. Shan, Role of LXRs in control of lipogenesis, Genes Dev. 14 (22) (2000) 2831–2838.
[7] E.T. Kase, B. Andersen, H.I. Nebb, A.C. Rustan, G.H. Thoresen, 22-Hydroxycholesterols regulate lipid metabolism differently than T0901317 in human myotubes, Biochim. Biophys. Acta 1761 (12) (2006) 1515–1522.
[8] T.A. Spencer, D. Li, J.S. Russel, J.L. Collins, R.K. Bledsoe, T.G. Consler, L.B. Moore, C.M. Galardi, D.D. McKee, J.T. Moore, M.A. Watson, D.J. Parks, M.H. Lambert, T.M. Willson, Pharmacophore analysis of the nuclear oxysterol receptor LXRalpha, J. Med. Chem. 44 (6) (2001) 886–897.
[9] N. Terasaka, A. Hiroshima, T. Koieyama, N. Ubukata, Y. Morikawa, D. Nakai, T. Inaba, T-0901317, a synthetic liver X receptor ligand, inhibits development of atherosclerosis in LDL receptor-deficient mice, FEBS Lett. 536 (1–3) (2003) 6–11.
[10] A. Grefhorst, T.H. van Dijk, A. Hammer, F.H. van der Sluijs, R. Havinga, L.M. Havekes, J.A. Romijn, P.H. Groot, D.J. Reijngoud, F. Kuipers, Differential effects of pharmacological liver X receptor activation on hepatic and peripheral insulin sensitivity in lean and ob/ob mice, Am. J. Physiol. Endocrinol. Metab. 289 (5) (2005) E829–E838.
[11] C. Lara-Castro, W.T. Garvey, Intracellular lipid accumulation in liver and muscle and the insulin resistance syndrome, Endocrinol. Metab. Clin. North Am. 37 (4) (2008) 841–856.
[12] E. Fabbrini, F. Magkos, B.S. Mohammed, T. Pietka, N.A. Abumrad, B.W. Patterson, A. Okunade, S. Klein, Intrahepatic fat, not visceral fat, is linked with metabolic complications of obesity, Proc. Natl. Acad. Sci. U. S. A. 106 (36) (2009) 15430–15435.
[13] E.T Kase, G.H. Thoresen, S. Westerlund, K. Hojlund, A.C. Rustan, M. Gaster, Liver X receptor antagonist reduces lipid formation and increases glucose metabolism in myotubes from lean, obese and type 2 diabetic individuals, Diabetologia 50 (10) (2007) 2171–2180.
[14] P. Kotokorpi, E. Ellis, P. Parini, L.M. Nilsson, S. Strom, K.R. Steffensen, J.A. Gustafsson, A. Mode, Physiological differences between human and rat primary hepatocytes in response to liver X receptor activation by 3-[3-[N-(2-chloro-3-trifluoromethylbenzyl)-(2 2-diphenylethyl)amino]propyl oxy]phenylacetic acid hydrochloride (GW3965), Mol. Pharmacol. 72 (4) (2007) 947–955.
[15] R. Abagyan, M. Totrov, D. Kuznetsov, Icm—a new method for protein modeling and design—applications to docking and structure prediction from the distorted native conformation, J. Comput. Chem. 15 (5) (1994) 488–506.
[16] M. Gaster, S.R. Kristensen, H. Beck-Nielsen, H.D. Schroder, A cellular model system of differentiated human myotubes, APMIS 109 (11) (2001) 735–744.
[17] M. Wabitsch, R.E. Brenner, I. Melzner, M. Braun, P. Moller, E. Heinze, K.M. Debatin, H. Hauner, Characterization of a human preadipocyte cell strain with high capacity for adipose differentiation, Int. J. Obes. Relat. Metab. Disord. 25 (1) (2001) 8–15.
[18] T. Ranheim, A. Gedde-Dahl, A.C. Rustan, C.A. Drevon, Fatty acid uptake and metabolism in CaCo-2 cells: eicosapentaenoic acid (20:5(*n*-3)) and oleic acid (18:1(*n*-9)) presented in association with micelles or albumin, Biochim. Biophys. Acta 1212 (3) (1994) 295–304.
[19] N.P. Hessvik, S.S. Bakke, K. Fredriksson, M.V. Boekschoten, A. Fjorkenstad, G. Koster, M.K. Hesselink, S. Kersten, E.T. Kase, A.C. Rustan, G.H. Thoresen, Metabolic switching of human myotubes is improved by *n*-3 fatty acids, J. Lipid Res. 51 (8) (2010) 2090–2104.
[20] M.M. Bradford, A rapid and sensitive method for the quantitation of microgram quantities of protein utilizing the principle of protein–dye binding, Anal. Biochem. 72 (1976) 248–254.
[21] A.J. Wensaas, A.C. Rustan, K. Lovstedt, B. Kull, S. Wikstrom, C.A. Drevon, S. Hallen, Cell based multiwell assays for detection of substrate accumulation and oxidation, J. Lipid Res. 48 (2007) 961–967.
[22] N.P. Hessvik, M.V. Boekschoten, M.A. Baltzersen, S. Kersten, X. Xu, H. Andersen, A.C. Rustan, G.H. Thoresen, LXR{beta} is the dominant LXR subtype in skeletal muscle regulating lipogenesis and cholesterol efflux, Am. J. Physiol. Endocrinol. Metab. 298 (3) (2010) E602–E613.
[23] S. Svensson, T. Ostberg, M. Jacobsson, C. Norstrom, K. Stefansson, D. Hallen, I.C. Johansson, K. Zachrisson, D. Ogg, L. Jendeberg, Crystal structure of the heterodimeric complex of LXRalpha and RXRbeta ligand-binding domains in a fully agonistic conformation, EMBO J. 22 (18) (2003) 4625–4633.
[24] E.T. Kase, A.J. Wensaas, V. Aas, K. Hojlund, K. Levin, G.H. Thoresen, H. Beck-Nielsen, A.C. Rustan, M. Gaster, Skeletal muscle lipid accumulation in type 2 diabetes may involve the liver X receptor pathway, Diabetes 54 (4) (2005) 1108–1115.
[25] K.J. Livak, T.D. Schmittgen, Analysis of relative gene expression data using real-time quantitative PCR and the 2(-Delta Delta C(T)) Method, Methods 25 (4) (2001) 402–408.
[26] L.O. Li, J.M. Ellis, H.A. Paich, S. Wang, N. Gong, G. Altshuller, R.J. Thresher, T.R. Koves, S.M. Watkins, D.M. Muoio, G.W. Cline, G.I. Shulman, R.A. Coleman, Liver-specific loss of long chain acyl-CoA synthetase-1 decreases triacylglycerol synthesis and beta-oxidation and alters phospholipid fatty acid composition, J. Biol. Chem. 284 (41) (2009) 27816–27826.
[27] Y.L. Wang, W. Guo, Y. Zang, G.C. Yaney, G. Vallega, L. Getty-Kaushik, P. Pilch, K. Kandror, B.E. Corkey, Acyl coenzyme A synthetase regulation: putative role in long-chain acyl coenzyme A partitioning, Obes. Res. 12 (11) (2004) 1781–1788.
[28] Y. Zhou, P. Abidi, A. Kim, W. Chen, T.T. Huang, F.B. Kraemer, J. Liu, Transcriptional activation of hepatic ACSL3 and ACSL5 by oncostatin m reduces hypertriglyceridemia through enhanced beta-oxidation, Arterioscler. Thromb. Vasc. Biol. 27 (10) (2007) 2198–2205.
[29] T. Fujino, M.J. Kang, H. Suzuki, H. Iijima, T. Yamamoto, Molecular characterization and expression of rat acyl-CoA synthetase 3, J. Biol. Chem. 271 (28) (1996) 16748–16752.
[30] D.E. Kelley, L.J. Mandarino, Fuel selection in human skeletal muscle in insulin resistance: a reexamination, Diabetes 49 (5) (2000) 677–683.
[31] D.E. Kelley, Skeletal muscle fat oxidation: timing and flexibility are everything, J. Clin. Invest. 115 (7) (2005) 1699–1702.
[32] B. Ukropcova, M. McNeil, O. Sereda, L. de Jonge, H. Xie, G.A. Bray, S.R. Smith, Dynamic changes in fat oxidation in human primary myocytes mirror metabolic characteristics of the donor, J. Clin. Invest. 115 (7) (2005) 1934–1941.
[33] L.K. Juvet, S.M. Andresen, G.U. Schuster, K.T. Dalen, K.A. Tobin, K. Hollung, F. Haugen, S. Jacinto, S.M. Ulven, K. Bamberg, J.A. Gustafsson, H.I. Nebb, On the role of liver X receptors in lipid accumulation in adipocytes, Mol. Endocrinol. 17 (2) (2003) 172–182.
[34] T. Yoshikawa, H. Shimano, M. Amemiya-Kudo, N. Yahagi, A.H. Hasty, T. Matsuzaka, H. Okazaki, Y. Tamura, Y. Iizuka, K. Ohashi, J. Osuga, K. Harada, T. Gotoda, S. Kimura, S. Ishibashi, N. Yamada, Identification of liver X receptor-retinoid X receptor as an activator of the sterol regulatory element-binding protein 1c gene promoter, Mol. Cell Biol. 21 (9) (2001) 2991–3000.
[35] S.B. Joseph, B.A. Laffitte, P.H. Patel, M.A. Watson, K.E. Matsukuma, R. Walczak, J.L. Collins, T.F. Osborne, P. Tontonoz, Direct and indirect mechanisms for regulation of fatty acid synthase gene expression by liver X receptors, J. Biol. Chem. 277 (13) (2002) 11019–11025.
[36] D.E. Kelley, B. Goodpaster, R.R. Wing, J.A. Simoneau, Skeletal muscle fatty acid metabolism in association with insulin resistance, obesity, and weight loss, Am. J. Physiol. 277 (6 Pt 1) (1999) E1130–E1141.
[37] E.E. Blaak, D.P. van Aggel-Leijssen, A.J. Wagenmakers, W.H. Saris, M.A. van Baak, Impaired oxidation of plasma-derived fatty acids in type 2 diabetic subjects during moderate-intensity exercise, Diabetes 49 (12) (2000) 2102–2107.
[38] M. Gaster, A.C. Rustan, V. Aas, H. Beck-Nielsen, Reduced lipid oxidation in skeletal muscle from type 2 diabetic subjects may be of genetic origin: evidence from cultured myotubes, Diabetes 53 (3) (2004) 542–548.
[39] A.J. Wensaas, A.C. Rustan, M. Just, R.K. Berge, C.A. Drevon, M. Gaster, Fatty acid incubation of myotubes from humans with type 2 diabetes leads to enhanced release of beta-oxidation products because of impaired fatty acid oxidation: effects of tetradecylthioacetic acid and eicosapentaenoic acid, Diabetes 58 (3) (2009) 527–535.
[40] K. Aravindhan, C.L. Webb, M. Jaye, A. Ghosh, R.N. Willette, N.J. DiNardo, B.M. Jucker, Assessing the effects of LXR agonists on cellular cholesterol handling: a stable isotope tracer study, J. Lipid Res. 47 (6) (2006) 1250–1260.
[41] S. Murthy, E. Born, S.N. Mathur, F.J. Field, LXR/RXR activation enhances basolateral efflux of cholesterol in CaCo-2 cells, J. Lipid Res. 43 (7) (2002) 1054–1064.
[42] S.P. Zhao, B.L. Yu, X.Z. Xie, S.Z. Dong, J. Dong, Dual effects of oxidized low-density lipoprotein on LXR-ABCA1-apoA-I pathway in 3T3-L1 cells, Int. J. Cardiol. 128 (1) (2008) 42–47.
[43] B.L. Wagner, A.F. Valledor, G. Shao, C.L. Daige, E.D. Bischoff, M. Petrowski, K. Jepsen, S.H. Baek, R.A. Heyman, M.G. Rosenfeld, I.G. Schulman, C.K. Glass, Promoter-specific roles for liver X receptor/corepressor complexes in the regulation of ABCA1 and SREBP1 gene expression, Mol. Cell Biol. 23 (16) (2003) 5780–5789.

[44] F. Morello, E. Saglio, A. Noghero, D. Schiavone, T.A. Williams, A. Verhovez, F. Bussolino, F. Veglio, P. Mulatero, LXR-activating oxysterols induce the expression of inflammatory markers in endothelial cells through LXR-independent mechanisms, Atherosclerosis 207 (1) (2009) 38–44.
[45] I. Bjorkhem, Are side-chain oxidized oxysterols regulators also in vivo? J. Lipid Res. 50 (Suppl.) (2009) S213–S218.
[46] K.A. Houck, K.M. Borchert, C.D. Hepler, J.S. Thomas, K.S. Bramlett, L.F. Michael, T.P. Burris, T0901317 is a dual LXR/FXR agonist, Mol. Genet Metab. 83 (1–2) (2004) 184–187.
[47] N. Kumar, L.A. Solt, J.J. Conkright, Y. Wang, M.A. Istrate, S.A. Busby, R.D. Garcia-Ordonez, T.P. Burris, P.R. Griffin, The benzenesulfoamide T0901317 [N-(2,2,2-trifluoroethyl)-N-[4-[2,2,2-trifluoro-1-hydroxy-1-(trifluoromethyl)ethyl]phenyl]-benzenesulfonamide] is a novel retinoic acid receptor-related orphan receptor-alpha/gamma inverse agonist, Mol. Pharmacol. 77 (2) (2010) 228–236.
[48] N. Mitro, L. Vargas, R. Romeo, A. Koder, E. Saez, T0901317 is a potent PXR ligand: implications for the biology ascribed to LXR, FEBS Lett. 581 (9) (2007) 1721–1726.